Tissue and Cell 93 (2025) 102644

Contents lists available at ScienceDirect

Tissue and Cell

journal homepage: www.elsevier.com/locate/tice

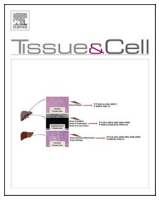

Immunohistochemical assessment of ERM proteins (ezrin, radixin, moesin) in the ovaries of different species

Natascha Leitner [a], Ismi Simsek [a], Juraj Hlavaty [a], Sabine Schäfer-Somi [b], Ingrid Walter [a,c,*]

[a] Department of Biomedical Sciences and Pathobiology, Center of Pathobiology, University of Veterinary Medicine, Vienna, Austria
[b] Department of Small Animals and Horses, Clinical Center for Reproduction University of Veterinary Medicine, Vienna, Austria
[c] VetCore Facility for Research, University of Veterinary Medicine, Vienna, Austria

ARTICLE INFO

Keywords:
ERM proteins
Ovary
Follicle
Immunohistochemistry

ABSTRACT

The ezrin/radixin/moesin proteins play a central role in cross-linking plasma membrane proteins with the actin cytoskeleton. Despite intensive ERM protein research in many tissues and pathologies, little is known about these proteins in healthy tissues of reproductive organs. Therefore, we examined ezrin, phosphorylated ezrin/radixin/moesin (pan-pERM), radixin, and moesin distribution at the cellular level by means of immunohistochemistry in ovaries of the following animal species: mouse, dog, cat, sheep, pig, horse, and cynomolgus monkey. Ezrin was expressed in oocytes, ovarian surface, granulosa cells and corpus luteum. A characteristic, predominantly membranous pan-pERM staining pattern was observed in ovarian surface epithelium, oocyte, granulosa cells and corpus luteum. Moesin immunoreactivity was present in all ovarian structures with a prominent signal in endothelial cells of blood vessels. Oocytes, granulosa cells and corpus luteum revealed mainly nuclear radixin staining. Staining pattern and subcellular localization (membranous, cytoplasmic, nuclear) varied between different animal species and between particular ERM proteins as well. This data may help gain new insights into the physiological function of ERM proteins in biological events in the female reproductive system.

1. Introduction

Ezrin/radixin/moesin (ERM) is a family of proteins that have been widely studied in the context of neoplasms, in particular their role in cell proliferation, migration, invasion, and the metastatic process has been observed (Horwitz et al., 2016; Demacopulo et al., 2016; Hlavatý et al., 2017; Barik et al., 2022). ERM family members ezrin, radixin, and moesin possess common structural characteristics. They consist of three major domains: the amino-terminal FERM domain, a central α-helical domain, and a carboxy-terminal ERM association domain (reviewed in Barik et al., 2022; Ponuwei, 2016). These three paralog proteins display high sequence homology, especially at their FERM domains (Tsukita and Yonemura, 1999; Michie et al., 2019). However, whereas ezrin and moesin exist as a single isoform, radixin is expressed in various isoforms (Michie et al., 2019).

In the cytoplasm, inactive ERM proteins build a loop (head to tail, closed conformation). Once activated by phosphorylation, they undergo a conformational change (open conformation), and the molecule connects to a transmembrane receptor with its amino-terminal domain, and with the actin cytoskeleton with its carboxy-terminal domain. In this conformation ezrin acts as a signal transmitter and can now regulate several signal transduction pathways (reviewed in Barik et al., 2022). ERM proteins are also essential during mitotic cell division (shape, cortical structure, spindle orientation) (Fehon et al., 2010).

Members of the ERM protein family have been described in context of ovarian cancer (Demacopulo et al., 2016) and granulosa cell tumours in humans (Wan et al., 2021). Ezrin has been verified to be a prognostic marker in human ovarian cancer (Horwitz et al., 2016; Köbel et al., 2006a), endometrial cancer (Köbel et al., 2006b), breast carcinoma (Storr et al., 2023), osteosarcoma (Li et al., 2013), prostate cancer (Chen et al., 2022) and various other cancers (reviewed in Barik et al., 2022), while moesin was found to be a possible prognostic marker in human breast cancer (Yu et al., 2019) and gastric adenocarcinoma (Jung et al., 2013). For radixin, a possible prognostic role was found in association with microRNA-31 downregulation in glioma (Wang et al., 2014). Ovarian tumours do occur in domestic animal species as well, although in a different matter concerning malignancy (reviewed in MacLachlan, 1987). Dolin et al (Dolin et al., 2023). showed a high expression of ezrin

* Correspondence to: Center of Pathobiology, University of Veterinary Medicine, Veterinaerplatz 1, Vienna A-1210, Austria.
E-mail addresses: natascha.leitner@vetmeduni.ac.at (N. Leitner), ismi.simsek@gmx.at (I. Simsek), Juraj.hlavaty@vetmeduni.ac.at (J. Hlavaty), sabine.schaefer@vetmeduni.ac.at (S. Schäfer-Somi), Ingrid.walter@vetmeduni.ac.at (I. Walter).

https://doi.org/10.1016/j.tice.2024.102644
Received 8 July 2024; Received in revised form 26 November 2024; Accepted 26 November 2024
Available online 30 November 2024

in a horse granulosa cell tumor, while the proliferation rate in the respective region was low.

Even though widely observed in cancer research, there is less data concerning these proteins in healthy tissues and organs, in particular for the ovary and other reproductive organs. Scattered information about ezrin protein in the healthy ovary (Chen et al., 2001), ovarian surface epithelium (Fadiel et al., 2012) or oocytes in mice (Cohen et al., 2022) is available. The ovary is an organ with a high grade of remodelling events. The series of follicle stage development starts with the primordial follicles which are characterised by an oocyte surrounded by a single layer of flat epithelial cells. Primordial follicles with a cuboidal epithelium are the next stages, followed by secondary (pre-antral) follicles with a growing oocyte that develops a zona pellucida and a squamous follicular epithelium. During the secondary follicle stage, the theca emerges from the surrounding connective tissue. Finally, a tertiary follicle with an antrum lined by granulosa cells and a fully developed theca is present. However, no systematic investigation exists about the presence of ERM proteins in the ovary and its specific structures such as praeantral and antral follicles, corpus luteum, stroma/theca cells, ovarian surface epithelium, and blood vessels. This data is needed to clarify the physiologic functions of ERM proteins in healthy tissue and serve as an important basis for the judgement of alterations during neoplastic or other pathologic processes.

A major aspect that should be addressed regarding ERM proteins in the ovary, is the structure of the corpus luteum. In most species, the corpus luteum develops from theca interna cells (stromal cells involved in steroid hormone production) and granulosa cells. These cells "luteinize", meaning hypertrophy of cells, storage of lipids, and angiogenesis take place simultaneously. During its development, the corpus luteum shares several similarities with neoplastic processes such as cell proliferation, migration, angiogenesis, and remodeling (Smith et al., 1994). We hypothesise that ERM proteins have a distinct role in follicle growth and corpus luteum development in the ovary. The aim of this investigation was to elucidate the distribution of ERM proteins in various structures of a healthy ovary at the cellular level. To support and strengthen the biological significance of our findings, we investigated ovaries of different species. We examined ezrin, p-ezrin, radixin, and moesin in histological sections of ovaries of mouse, dog, cat, sheep, pig, horse, and monkey (cynomolgus, *Macaca fascicularis*) by means of immunohistochemistry.

2. Material and methods

2.1. Tissue samples

Formalin-fixed, paraffin embedded (FFPE) ovaries and fresh frozen control tissue (kidneys, ovaries) were obtained from archive material of the VetBiobank (Walter et al., 2020) or collected during necropsy or therapeutical medical intervention according to the ethical standards and rules at the Vetmeduni Vienna. Ovarian sections from three individuals of each species (cat, dog, pig, sheep, mouse, horse, monkey), free of signs of pathohistological alterations, were examined for the presence of follicular stages and/or corpus luteum. Hemalum Eosin (H&E)-stained sections (Romeis, 1989) were used for general assessment of ovarian structures.

For immunohistochemistry, samples were fixed in 4 % neutral buffered formaldehyde (Liquid Production GmbH, Flintsbach am Inn, Germany) and paraffin embedded. For western blot analyses, samples were lysed in RIPA buffer (50 mM Tris–HCl pH 7.4, 500 mM NaCl, 0.5 % sodium deoxycholate (all Carl Roth GmbH, Karlsruhe, Germany), 1 % Nonidet P-40 (Igepal, Sigma Aldrich, St. Louis, MO, USA), 0.1 % sodium dodecyl sulphate (Serva, Mannheim, Germany) supplemented with 1 % protease and phosphatase inhibitors (Protease Inhibitor Cocktail and Phosphatase Inhibitor Cocktail 3; both Sigma Aldrich) and supernatant fraction was stored at −80°C until further processing.

2.2. Immunohistochemistry

Paraffin embedded (FFPE) specimens were cut at 3 μm and rehydrated. In order to block endogenous peroxidases, samples were incubated 15 min at room temperature in 0.6 % H_2O_2 in methanol (Carl Roth). All antigen retrievals were done at 85°C for 30 min in 0.01 M citrate buffer at pH6.0, except for the protocol from moesin were Tris-EDTA at pH9 was used under the same conditions, followed by washing steps (2x5min) at pH7.4 in PBS. Incubation with the respective primary antibody (dilutions and antibodies see Table 1) was performed over night at 4°C after protein block with normal goat serum (Sigma Aldrich, St. Louis, MO, USA) for 30 min at room temperature. After another washing step in PBS (2x5min), the slices were incubated with anti-rabbit secondary antibody labelled to horse-radish-peroxidase for 30 min (BrightVision Poly-HRP-anti-rabbit, ImmunoLogic, Duiven, The Netherlands) and after a washing step in PBS with DAB-Solution for development of staining (3′3'diaminobenzidine, Richard Allen Scientific, San Diego, CA, USA). Next, samples were washed in distilled water and nuclei counterstained for 3 min in Mayer's hemalum (Romeis, 1989), followed by dehydration and mounting with DPX (Sigma Aldrich). Evaluation was performed using an Olympus BX53 microscope (Olympus, Vienna, Austria).

2.3. Western blot

To support immunohistochemistry results, a species-specificity test with positive control tissue (kidney/ovary) was made by western blot. Fresh frozen monkey tissue was not available; therefore, western blotting experiments were not performed for this species.

Protein concentrations of the lysed samples were calculated using DC™ Protein Assay (BioRad, Hercules, CA, USA) according to the manufacturer's protocol. Per lane and sample twenty microgram of protein extracts were loaded on a 10 % polyacrylamide gel for electrophoresis (SDS-PAGE, reducing conditions) with BioRad Mini Protean Tetra System (BioRad), transferred to a PVDF membrane (GE Healthcare, Chicago, IL, USA) and blocked for 2 h with Western Blocking Reagent (Roche, Basel, Switzerland) diluted 1:10 in TBST to inhibit unspecific binding of the antibody. Afterward membranes were incubated over night at 4°C with the respective primary antibody diluted in Western Blocking Reagent/TBST (dilutions and antibodies see Table 1). Thereafter, membranes were washed 5x8min in TBST and incubated for 30 min with the secondary antibody (ECL™ Anti-rabbit IgG, HRP-linked whole antibody; GE Healthcare; dilution 1:5 000 in Western Blocking Reagent/TBST) at room temperature. This procedure was followed by further washing steps (4x8min TBST and finally 1x8min TBS) and signal detection using BioRad ChemiDoc Image System with Image Lab Software (BioRad) and ECL Western Blot Detection Reagents (GE Healthcare, Chicago, IL, USA).

3. Results

Immunohistochemistry revealed positive signals in all species assessed. Several attempts were made to control specificity of applied antibodies for the range of species examined (cat, dog, pig, sheep, mouse, horse, monkey). Positive control tissue sections (kidney, Supplementary Figure 1) of respective species revealed expected staining patterns assuming its comparability to human tissue (The Human Protein Atlas, https://www.proteinatlas.org/). Negative controls, where the primary antibody was substituted by PBS, were blank; no unspecific binding of the secondary antibody system was observed in any species (data not shown). Western blotting experiments with respective control tissues (kidney) verified that applied antibodies were reactive with respective proteins of the analysed species (Supplementary Figure 2). The only exception was the absence of a positive signal for radixin in the sheep tissue lysate. Fresh tissue from cynomolgus monkey was not available, therefore, we cannot provide western blotting results for this

Table 1
List of primary antibodies used for immunohistochemistry and western blot detection.

Antibody name	Antibody types	Source	Catalogue nr.	Application	Dilution
Anti-EZR	rabbit polyclonal	Sigma Prestige, St. Louis, MO, USA	HPA021616	IHC	1:500
				WB	1:2 000
Phospho-ezrin (Thr567)/Radixin (Thr564)/Moesin (Thr558) (48G2)	rabbit monoclonal	Cell Signaling, Danvers, MA, USA	3726	IHC	1:800
Phospho-ezrin (Thr567)/Radixin (Thr564)/Moesin (Thr558) (41A3)	rabbit monoclonal	Cell Signaling, Danvers, MA, USA 5	3149	WB	1:500
Anti-radixin	rabbit polyclonal	Sigma Aldrich, St. Louis, MO, USA	R3653	IHC	1:1 000
				WB	1:1 600
Anti-moesin [EP1863Y]	rabbit monoclonal	Abcam, Cambridge, UK	Ab52490	IHC	1:800
				WB	1:500

IHC – Immunohistochemistry; WB – western blot

species. As the antibodies were declared to work on human tissue, a specific reactivity for monkey tissue is most likely. Blast analysis using scoring matrix BLOSUM 62 (Clone Manager 9, SciEd Software LLC, Westminster Colorado USA) revealed high protein similarity between human and cynomolgus ERM proteins (99 % in ezrin and radixin, 100 % in moesin). Not all structures (follicle stages, oocytes) were present in sections of horse ovaries, therefore, it was not possible to assess all immunohistochemical staining patterns in this species.

Ezrin immunohistochemistry revealed a similar staining pattern of most ovarian structures across analysed species (Fig. 1). The ovarian surface epithelium was positive in all species, in some specimens (cat, mouse) a signal was evident at the apical membrane. Oocytes were (cytoplasmic) stained in primordial, primary follicles of monkey, dog, cat, pig, sheep and mouse ovaries(Fig. 1a, d, g, j). The follicular epithelium was immunoreactive in all primordial, primary and secondary follicle stages and species, this was also true for granulosa cells in tertiary follicles (Fig. 1b, e, h, k). The staining pattern was partly cytoplasmic, partly membranous. Solely in mouse tissue, a nuclear staining pattern of the follicular epithelium/granulosa cells was observed (Fig. 1j, k). The immunostaining patterns for ezrin in the corpus luteum were quite different across the species: in the monkey, sheep, horse, and mouse tissue, a mosaic-like pattern of pronounced and moderately cytoplasmic stained lutein cells were observed (Fig. 1c, i, l). In monkey tissue, remarkably positive cells were distributed in a sparse pattern in the corpus luteum (Fig. 1c). Porcine specimens in addition revealed a membranous staining within the corpus luteum (Fig. 1i). Endothelia of blood vessels in the corpus luteum were marked by ezrin immunostaining, except in the mouse tissue (Fig. 1c, f, i, l). The stroma (area of theca) was positive after staining with anti-ezrin in all species (Fig. 1b, e, h, k).

Pan-phosphorylated ERM (pan-pERM) antibody cannot distinguish between p-ezrin Thr567, p-radixin Thr564 and p-moesin Thr558 by immunohistochemical analysis. The activated forms of these proteins, connecting the actin cytoskeleton to a transmembrane receptor, predominantly marked the membranes in follicular epithelium of primordial and primary follicles except in the mouse specimen (Fig. 2). In secondary and tertiary follicles, when the zona pellucida has already developed, pan-pERM staining was present on the oocyte surface (Fig. 2a, b, d, e, h, j, k). In the feline ovary, the immunoreactivity also included the area of the zona pellucida (Fig. 2e). The follicular epithelium in secondary and tertiary follicles (granulosa cells) showed a membranous staining, except in the mouse specimen (Fig. 2a, b, e, g, h, j, k). Other structures that were positive in all species (except mouse) included the surface epithelium, stroma, and corpus luteum. In the corpus luteum, all species (except mouse) showed membranous staining of lutein cells (Fig. 2c, f, i, l). Endothelial cells were marked by pan-pERM immunohistochemistry within and outside of the corpus luteum. The mouse tissue behaved quite distinctly after pan-pERM immunostaining, as beside the oocyte surface and endothelia of blood vessels, no other structures were stained (Fig. 2j, k, l).

Moesin immunoreactivity was observed in the follicle epithelium of primary and primordial follicles, surface epithelium and stroma in monkey tissue (Fig. 3a, b). In tertiary follicles in monkey ovary the surface area of the oocyte was marked; however, granulosa cells were not stained (Fig. 3b). In the feline ovary, moesin immunostaining was pronounced at the outside of the zona pellucida, the contact area of granulosa cells with the zona in secondary and tertiary follicles (Fig. 3d, e). In the other species (mouse, pig, sheep, and dog) no moesin immunoreactivity was detected in the oocyte and no staining of the granulosa cells was observed (Fig. 3g, h, j, k). Moesin staining in monkey ovary was present in the corpus luteum in the lutein cell membrane and endothelia of blood vessels (Fig. 3c). Membranous immunoreaction of lutein cells and endothelial cells was also observed in horse, pig and dog species (Fig. 3f, i); a predominant cytoplasmic staining was seen in the mouse lutein cells (Fig. 3l). Sheep and cat lutein cells showed no immunostaining for moesin. Blood vessel endothelia of all species except mouse were marked by moesin, in particular in the theca folliculi and the corpus luteum.

Radixin staining in ovarian tissue sections was present in follicle epithelium in primordial and primary follicles, surface epithelium and stroma in all species (Fig. 4). Signals for radixin were detected in secondary and tertiary follicle epithelium/granulosa cells as well as in the oocytes with cytoplasmic and nuclear localization (Fig. 4). The surface of the oocyte was marked in cat, dog and mouse specimens (Fig. 4d, e, j, k). Lutein cells showed cytoplasmic immunoreactivity in all species (Fig. 4c, f, i, l). In porcine blood vessels, endothelia were stained (Fig. 4i).

4. Discussion

Ezrin/radixin/moesin (ERM) proteins were identified as key players in cell signalling, morphogenesis, motility, and metastasis (Muriel et al., 2016; Schön et al., 2019), often they have been studied in association with tumours and tumour progression (Storr et al., 2023). Ezrin is probably the most studied protein of the ERM family and was originally described as an essential component of the microvilli of the kidney, placenta and intestine (Berryman et al., 1993). Proteins of the ERM family share a high homology of sequences, however individual ERM proteins may have specific and unique physiological functions in tissues as they were described to be differentially expressed. Astonishingly, data about ERM protein expression and functions in their physiological context in the ovary are rare. Knock-out mice would be a good model to study the roles of ERM proteins in various organs. However, conflicting effects of ERM knock-out on phenotypes in mice were reported. While Doi et al. (Doi et al., 1999) found only mild effects of moesin knock-outs, as it seemed to be compensated by other members of the ERM family such as ezrin or radixin, other authors described that ezrin knock-out mice did not survive past weaning due to intestinal epithelial defects meaning that specific protein expression is essential (Saotome et al., 2004). Nishimura et al. found no marked structural differences in the placenta between ezrin knock-out and wild type ezrin mice, however, ezrin knock-out mice exhibited significant fetal growth retardation

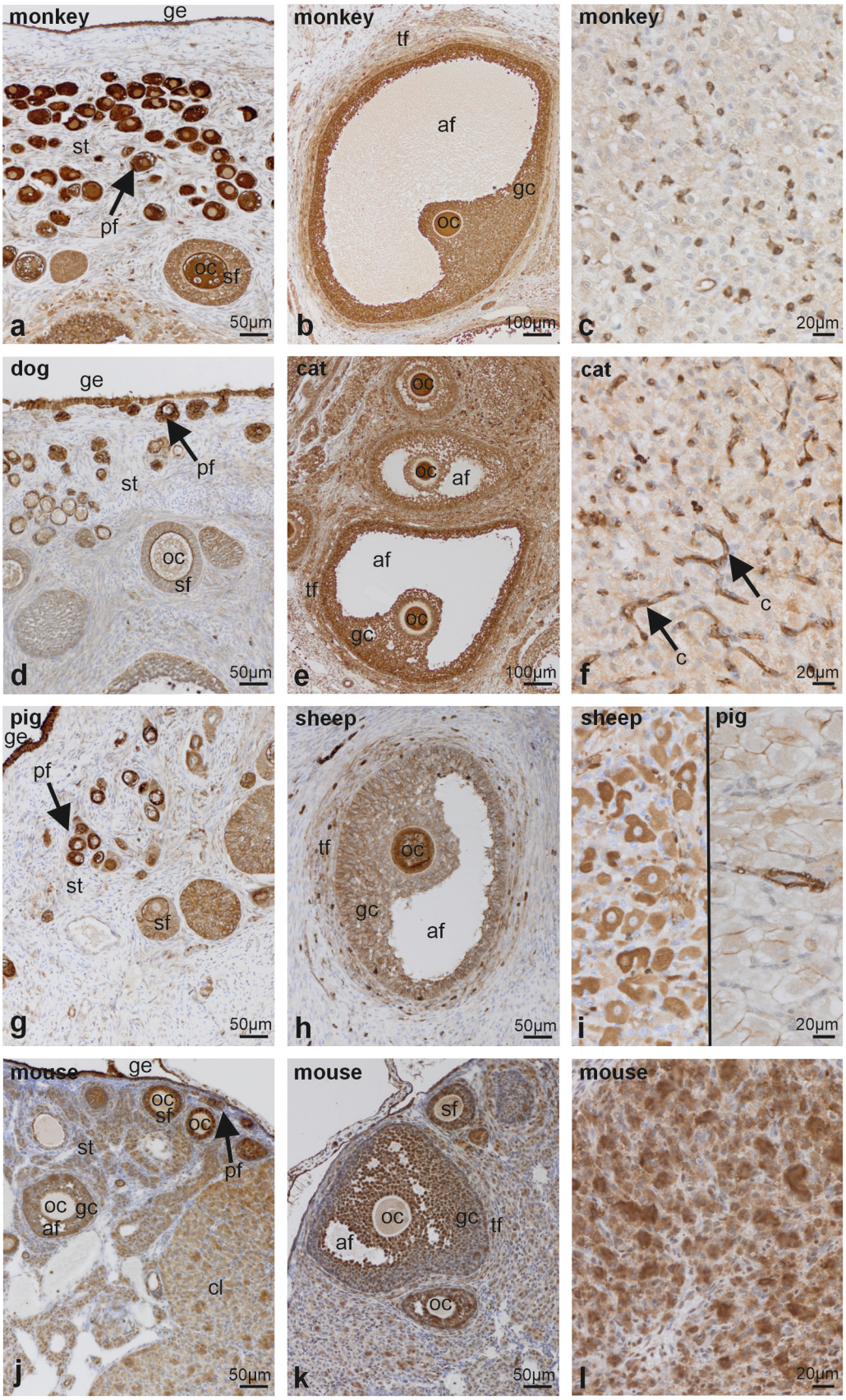

Fig. 1. Immunohistochemical detection of ezrin in different ovarian structures of monkey (a-c), dog (d), cat (e-f), pig (g), sheep (h-i), pig (i) and mouse (j-l). Ovarian surface epithelium and stroma with oocytes in preantral stages - primordial, primary, and secondary (a, d, g, j), tertiary follicle (b, e, h, k) and corpus luteum (c, f, i, l) are shown. af=antrum folliculi, c=capillary, ge=surface epithelium, gc=granulosa cells, oc=oocyte, pf=primordial follicles, sf=secondary follicle, tf=theca folliculi.

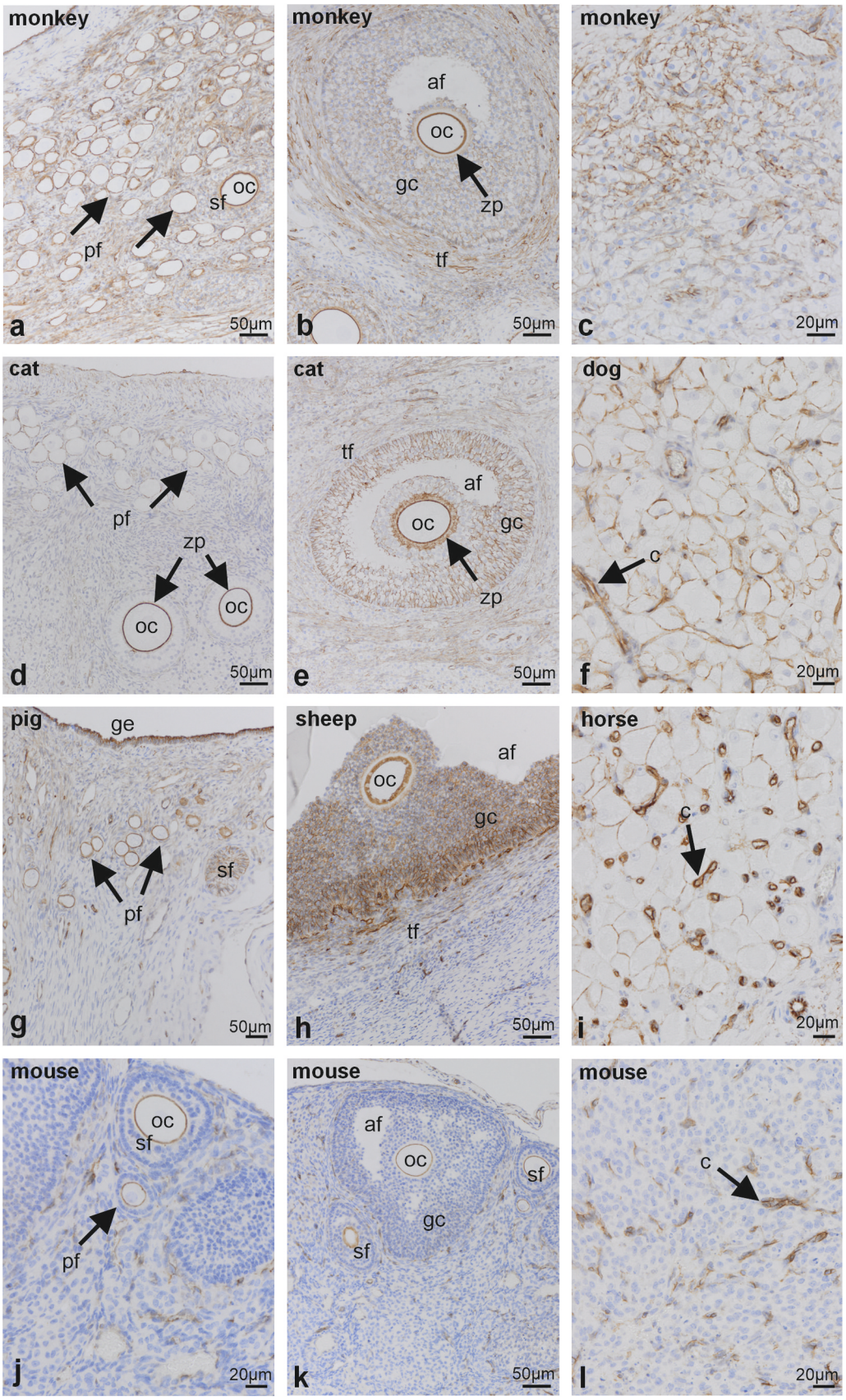

Fig. 2. Immunohistochemical detection of pan-pERM in different ovarian structures of monkey (a-c), cat (d-e), dog (f), pig (g), sheep (h), horse (i), and mouse (j-l). Ovarian surface epithelium and stroma with oocytes in diverse developmental stages - primordial, primary, and secondary (a, d, g, j), tertiary follicle (b, e, h, k) and corpus luteum (c, f, I, l) are shown. af=antrum folliculi, c=capillary, ge=surface epithelium, gc=granulosa cells, oc=oocyte, pf=primordial follicles, sf=secondars follicle, tf=theca folliculi, zp=zona pellucida.

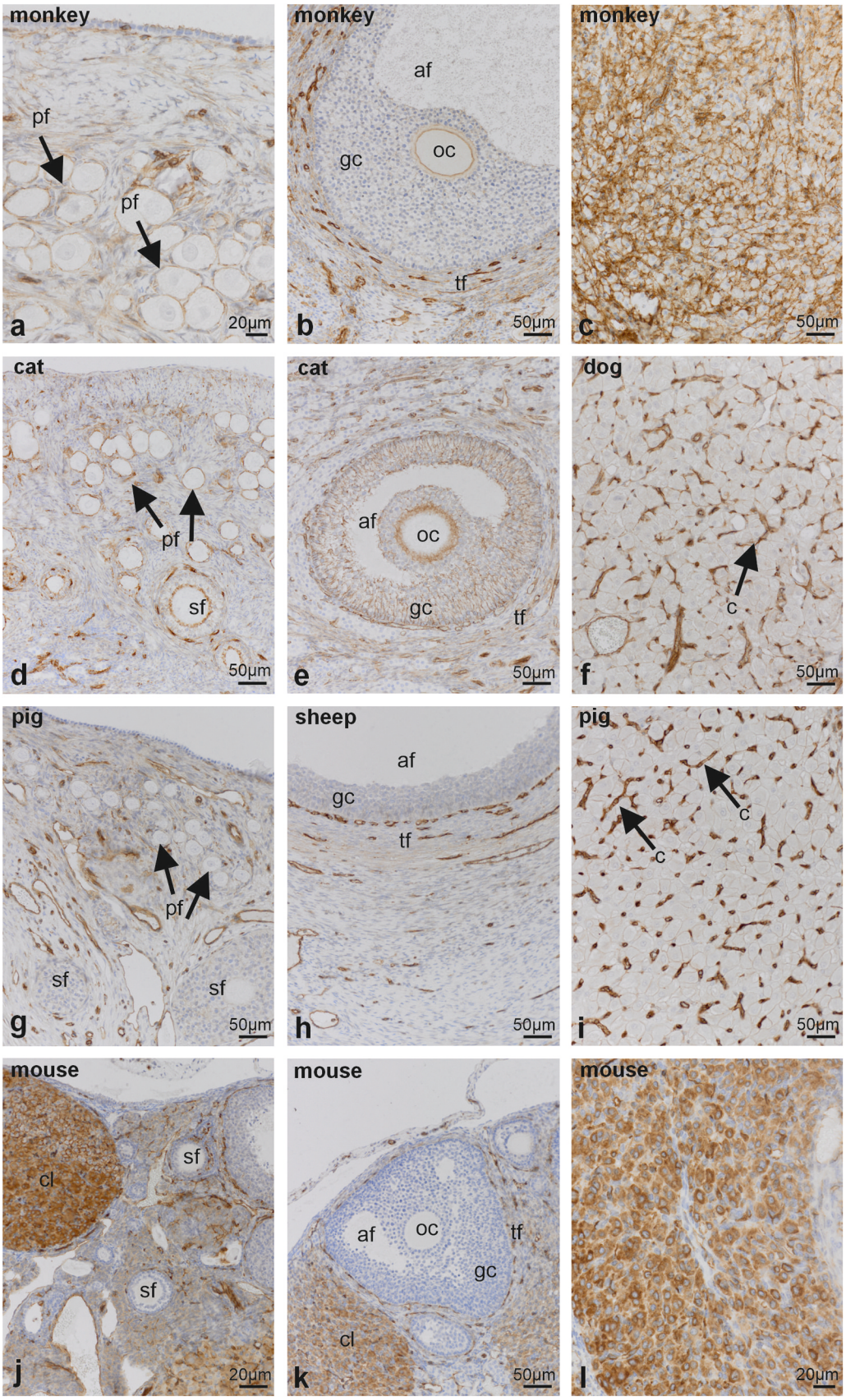

Fig. 3. Immunohistochemical detection of moesin in different ovarian structures of monkey (a-c), cat (d-e), dog (f), pig (g, i), sheep (h), mouse (j-l). Ovarian surface epithelium and stroma with oocytes in diverse developmental stages - primordial, primary, and secondary (a, d, g, j), tertiary follicle (b, e, h, k) and corpus luteum (c, f, i, l) are shown. af=antrum folliculi, c=capillary, cl=corpus luteum, ge=surface epithelium, gc=granulosa cells, oc=oocyte, pf=primordial follicles, tf=theca folliculi.

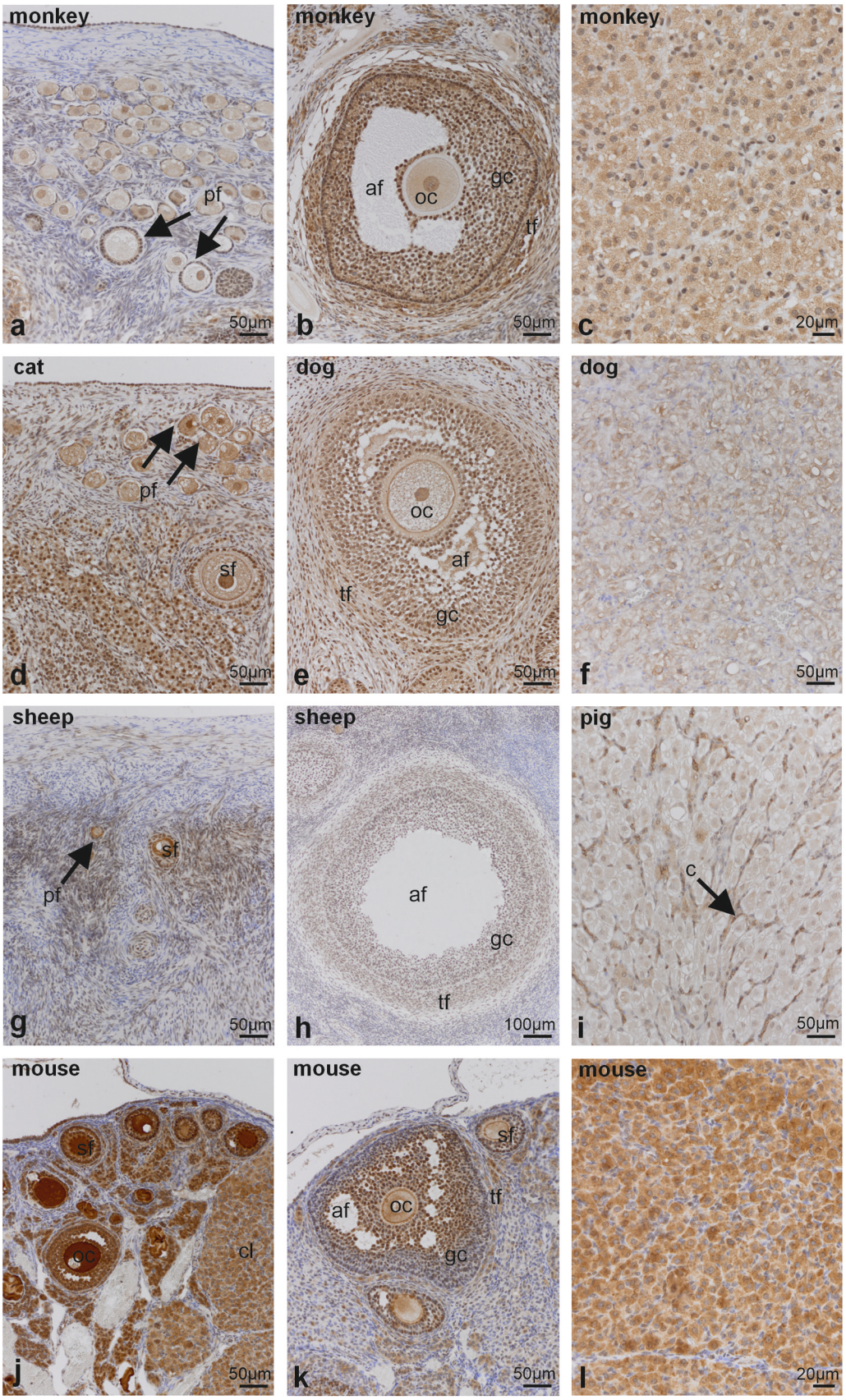

Fig. 4. Immunohistochemical detection of radixin in different ovarian structures of monkey (a-c), cat (d) dog (e, f), sheep (g, h), pig (i), and mouse (j-l). Ovarian surface epithelium and stroma with oocytes in diverse developmental stages - primordial, primary, and secondary (a, d, g, j), tertiary follicle (b, e, h, k) and corpus luteum (c, f, i, l) are shown. af=antrum folliculi, c=capillary, cl=corpus luteum, ge=surface epithelium, gc=granulosa cells, oc=oocyte, pf=primordial follicles, sf=secondary follicle, tf=theca folliculi.

(Nishimura et al., 2024). In functional experiments with human trophoblast cells, reduction of ezrin by siRNAs or a phosphorylation Thr567 inhibitor resulted in a significant reduction in both cell motility and cell invasion (Tabrizi et al., 2023). The exact role and essentiality of each ERM protein during the complex events of implantation, placentation and pregnancy requires further investigations.

Identification of ERM proteins in specific cell types in healthy organs might help elucidate the wide-ranged functions of the members of this protein family. In this context, the ovary with its unique physiological processes such as angiogenesis, cell proliferation, cell migration, and remodeling in the ovarian stroma, developing follicles and corpus luteum is an organ of the highest interest and, in some aspects, also shares similarities with tumours.

So far, data of healthy organs has mainly been gathered in comparison with neoplastic tissues, for example in breast cancer (Ghaffari et al., 2019). The presence and distribution of ERM proteins in the ovarian cells and compartments have not been assessed systematically. Chen et al. (Chen et al., 2001) analysed ezrin protein abundance in normal human ovaries by western blotting in parallel with ovarian cancer and found an overexpression in tumour specimens, however, also a clear signal in the normal ovarian tissue. Immunohistochemistry has not been done, therefore, ezrin expressing compartments and cell types have not been determined. For this purpose, immunohistochemistry is preferable over western blot or other methods with tissue lysis steps to identify the cell-specific distribution of ERM proteins within the ovary.

The **surface epithelium of the ovary** is a flat to prismatic, single layered epithelium that covers the ovarian surface and is involved in the process of follicle rupture and ovulation (Duffy et al., 2019). We demonstrated that the ovarian surface epithelium was characterised by a remarkable immunoreactivity for ezrin in all examined species. Also, the activated forms, phospho-ERM proteins, were found positive in all species, except mice. These results are partly in accordance with other reports (Gava et al., 2008) and partly in contrast with other findings (Fadiel et al., 2012), where the human ovarian surface epithelial cells were reported as negative. This discrepancy might be due to differences in ovarian surface areas or sexual cycle phases, as the specimens presented in Fadiel et al. (Fadiel et al., 2012) were either pre- or postmenopausal. The ovarian surface cell population is one source of neoplastic cells of human ovarian carcinomas (Zhang et al., 2019), therefore, the expression pattern and regulation of ERM proteins in this region should be a focus of further interest.

Oocytes are the only ovarian structures where ERM proteins have been studied, with the focus being mainly the surface of the oocytes. We detected ezrin and radixin in the oocyte cytoplasm and phosphorylated ERM proteins at the oocyte surface in all species. Several essential functions have been reported for ezrin in the oocyte. The formation of microvilli at the oocyte surface is fundamental for maintaining its structural stability and has been demonstrated to be dependent on ezrin and radixin expression (Zachos et al., 2008; Zhang et al., 2021). Furthermore, ERM proteins control actin cytoskeleton dynamics at various steps of oocyte maturation (Namgoong and Kim, 2016). Moesin has been described to be essential for the cortical actin cytoskeleton organization which is disrupted in moesin-depleted oocytes (Polesello et al., 2002). As moesin was only present on the oocyte surface in cat and monkey tissue, we suppose that other proteins of the ERM proteins can compensate for this function. ERM proteins are also responsible for the correct tension of the oocyte surface, which is a prerequisite for successful fertilisation (Cohen et al., 2022). After fertilisation, their presence increases, reflecting the dynamic changes that occur during oocyte developmental stages (Zhuan et al., 2022). In the present immunohistochemical investigation ERM proteins were detected in the cytoplasm and the surface of oocytes in all evaluated species. Therefore, it is concluded that they have an essential biological role during oocyte maturation.

Ezrin, pan-pERM and radixin proteins were present in the **follicle epithelium/granulosa cells** of preantral and antral follicle stages in all species, while moesin was only found in the monkey and cat species. During follicle development, epithelial cells proliferate to change from simple squamous to a simple prismatic and further to a stratified epithelium and contribute to the formation of the cumulus oophorus. Moreover, granulosa cells that surround the oocyte at the outside of the zona pellucida are in close contact with the oocyte surface via transzonal projections reaching through the zona pellucida (Roelen, 2020). It is likely, that the formation of these protrusions involves ERM proteins as cytoskeletal regulators.

After ovulation, a **corpus luteum** develops from the remaining granulosa cells in the Graafian follicle. In most species, stromal cells of the theca interna luteinize and contribute to corpus luteum formation. Proliferation, migration, angiogenesis, and remodeling are processes that take place during development of this endocrine structure. These match the processes which were described to involve ERM proteins in connection with tumour development (Fadiel et al., 2012). In the corpus luteum of the examined species, ERM proteins were differentially expressed in the lutein cells. In most species, there was a mosaic-like, differential immunostaining, in particular with anti-ezrin within the cells of the corpus luteum. We speculate that this pattern represents a different immunoreactivity of the larger (from granulosa cells) and smaller (from theca cells) lutein cells. However, specific markers for both cell types would be necessary to verify this assumption.

Angiogenesis, growth, and remodeling are major events during the cyclic alterations in the ovary and the development of the corpus luteum. These processes have been described to involve the action of ERM proteins, mostly in connection with neoplasms. However, these proteins will also be essential and active in comparable physiological processes. Ezrin, pan-pERM and moesin were clearly expressed in vascular endothelial cells of ovarian blood vessels in all assessed species. Ezrin was described to be a regulator of vascularization as knock down of ezrin reduced cell migration and angiogenesis capacity in human umbilical endothelial cells *in vitro* (Zhao et al., 2016). There was a strong reduction in the number of precapillary cords in human umbilical endothelial cells *in vitro* treated with specific ezrin-targeting siRNA, suggesting that ezrin is a key effector for cord formation. Similarly, moesin was reported to support angiogenesis in human aortic endothelial cells, having a stronger effect on tube formation than on sprouting (Degryse et al., 2017). Therefore, we assume that the presence of ERM proteins in the theca cells and corpus luteum will have a major role during vascular growth and angiogenesis.

5. Conclusion

The focus in ERM research was often at cancer research. According to the results of the present study, the wide expression of ERM proteins in structures of the normal ovary in various species should be considered when ovarian neoplasms are judged. More in-depth studies of ERM members in normal organs of different species will provide new insight into the broad physiological function of these proteins in biological events during reproduction and the understanding and treatment of ovarian diseases.

Ethics statement

This article does not contain any studies with human participants or laboratory animals. Analysed samples were obtained from archive material of the VetBiobank or collected during necropsy or therapeutical medical intervention according to the ethical standards and rules at the Vetmeduni Vienna.

Funding

This research did not receive any specific grant from funding agencies in the public, commercial, or not-for-profit sectors.

CRediT authorship contribution statement

Ismi Simsek: Visualization, Methodology, Investigation, Data curation. **Sabine Schäfer-Somi:** Writing – review & editing. **Juraj Hlavaty:** Writing – review & editing, Methodology, Formal analysis, Data curation. **Ingrid Walter:** Writing – review & editing, Visualization, Project administration, Formal analysis, Data curation, Conceptualization. **Natascha Leitner:** Writing – review & editing, Writing – original draft, Methodology, Investigation, Data curation.

Declaration of Generative AI and AI-assisted technologies in the writing process

For this article no AI assistance was used.

Declaration of Competing Interest

The authors have nothing to declare.

Acknowledgements

The authors cordially thank C. Höchsmann, B. Machac, O. Olszanska, and M. Wieser for their excellent technical support and Sara Aschauer for the design of the graphical abstract. This research was supported using resources of the VetCore Facility (VetImaging/VetBioBank) of the University of Veterinary Medicine Vienna.

Appendix A. Supporting information

Supplementary data associated with this article can be found in the online version at doi:10.1016/j.tice.2024.102644.

Data availability

Data will be made available on request.

References

Barik, G.K., Sahay, O., Paul, D., Santra, M.K., 2022. Ezrin gone rogue in cancer progression and metastasis: an enticing therapeutic target. Biochim Biophys. Acta Rev. Cancer 1877, 188753. https://doi.org/10.1016/j.bbcan.2022.188953.

Berryman, M., Franck, Z., Bretscher, A., 1993. Ezrin is concentrated in the apical microvilli of a wide variety of epithelial cells whereas moesin is found primarily in endothelial cells. J. Cell Sci. 105, 1025–1043. https://doi.org/10.1242/jcs.105.4.1025.

Chen, Z., Fadiel, A., Feng, Y., Ohtani, K., Rutherford, T., Naftolin, F., 2001. Ovarian epithelial carcinoma tyrosine phosphorylation, cell proliferation, and ezrin translocation are stimulated by interleukin 1 and epidermal growth factor. Cancer 92, 3068–3075. https://doi.org/10.1002/cncr.10149.

Chen, Z., Wang, J., Lu, Y., Lai, C., Qu, L., Zhuo, Y., 2022. Ezrin expression in circulating tumor cells is a predictor of prostate cancer metastasis. Bioengineered 13, 4076–4084. https://doi.org/10.1080/21655979.2021.2014710.

Cohen, J., Wang, L., Marques, S., Ialy-Radio, C., Barbaux, S., Lefèvre, B., Gourier, C., Ziyyat, A., 2022. Oocyte ERM and EWI proteins are involved in mouse fertilization. Front Cell Dev. Biol. 10, 863729. https://doi.org/10.3389/fcell.2022.863729.

Degryse, B., Britto, M., Shan, C.X., Wallace, R.G., Rochfort, K.D., Cummins, P.M., Meade, G., Murphy, R.P., 2017. Moesin and merlin regulate urokinase receptor-dependent endothelial cell migration, adhesion and angiogenesis. Int J. Biochem Cell Biol. 88, 14–22. https://doi.org/10.1016/j.biocel.2017.04.012.

Demacopulo, B., Lema, B.E., Cabrini, R.L., Kreimann, E.L., 2016. Similar expression pattern of NHERF1 and EZRIN in papillary but not solid areas of human serous ovarian carcinomas. Acta Histochem 118, 797–805. https://doi.org/10.1016/j.actahis.2016.10.002.

Doi, Y., Itoh, M., Yonemura, S., Ishihara, S., Takano, H., Noda, T., Tsukita, S., 1999. Normal development of mice and unimpaired cell adhesion/cell motility/actin-based cytoskeleton without compensatory up-regulation of ezrin or radixin in moesin gene knockout. J. Biol. Chem. 274, 2315–2321. https://doi.org/10.1074/jbc.274.4.2315.

Dolin, A., Schweiger, P., Waselau, M., Egerbacher, M., Walter, I., 2023. Immunohistochemical markers for equine granulosa cell tumors: a pilot study. J. Equine Sci. 34, 37–46. https://doi.org/10.1294/jes.34.37.

Duffy, D.M., Ko, C.M., Jo, M., Brannstrom, M., Curry Jr., T.E., 2019. Ovulation: parallels with inflammatory processes. Endocr. Rev. 40, 369–416. https://doi.org/10.1210/er.2018-00075.

Fadiel, A., Chen, Z., Ulukus, E., Ohtani, K., Hatami, M., Naftolin, F., 2012. Ezrin overexpression by transformed human ovarian surface epithelial cells, ovarian cleft cells, and serous ovarian adenocarcinoma cells. Reprod. Sci. 19, 797–805. https://doi.org/10.1177/1933719111433884.

Fehon, R.G., McClatchey, A.I., Bretscher, A., 2010. Organizing the cell cortex: the role of ERM proteins. Nat. Rev. Mol. Cell Biol. 11, 276–287. https://doi.org/10.1038/nrm2866.

Gava, N., Clarke, C.L., Bye, C., Byth, K., DeFazio, A., 2008. Global gene expression profiles of ovarian surface epithelial cells in vivo. J. Mol. Endocrinol. 40, 281–296. https://doi.org/10.1677/JME-07-0149.

Ghaffari, A., Hoskin, V., Turashvili, G., Varma, S., Mewburn, J., Mullins, G., Greer, P.A., Kiefer, F., Day, A.G., Madarnas, Y., SenGupta, S., Elliot, B.E., 2019. Intravital imaging reveals systemic ezrin inhibition impedes cancer cell migration and lymph node metastasis in breast cancer. Breast Cancer Res 21, 12. https://doi.org/10.1186/s13058-018-1079-7.

Hlavatý, J., Wolfesberger, B., Hauck, M., Obermayer-Pietsch, B., Fuchs-Baumgartinger, A., Miller, I., Walter, I., 2017. Ezrin and moesin expresion in canine and feline osteosarcoma. Histol. Histopathol. 32, 805–816. https://doi.org/10.14670/HH-11-848.

Horwitz, V., Davidson, B., Stern, D., Tropé, C.G., Tavor Re'em, T., Reich, R., 2016. Ezrin is associated with disease progression in ovarian carcinoma. PLoS ONE 11, e0162502. https://doi.org/10.1371/journal.pone.0162502.

Jung, W.Y., Kang, Y., Lee, H., Mok, Y.-J., Kim, H.K., Kim, A., Kim, B.-H., 2013. Expression of moesin and CD44 is associated with poor prognosis in gastric adenocarcinoma. Histopathology 63, 474–481. https://doi.org/10.1111/his.12202.

Köbel, M., Gradhand, E., Zeng, K., Schmitt, W.D., Kriese, K., Lantzsch, T., Wolters, M., Dittmer, J., Strauss, H.G., Thomssen, C., Hauptmann, S., 2006a. Ezrin promotes ovarian carcinoma cell invasion and its retained expression predicts poor prognosis in ovarian carcinoma. Int J. Gynecol. Pathol. 25, 121–130. https://doi.org/10.1097/01.pgp.0000185410.39050.ac.

Köbel, M., Langhammer, T., Hüttelmaier, S., Schmitt, W.D., Kriese, K., Dittmer, J., Strauss, H.-G., Thomssen, C., Hauptmann, S., 2006b. Ezrin expression is related to poor prognosis in FIGO stage I endometrioid carcinomas. Mod. Pathol. 19, 581–587. https://doi.org/10.1038/modpathol.3800567.

Li, H., Min, D., Zhao, H., Wang, Z., Zheng, Qui W., Tang, S., He, L., Sun, A., Yao, Y., Shen, Y., 2013. Z. The prognostic role of ezrin immunoexpression in osteosarcoma: a meta-analysis of published data. PLoS One 8, e64513. https://doi.org/10.1371/journal.pone.0064513.

MacLachlan, N.J., 1987. Ovarian disorders in domestic animals. Environ. Health Perspect. 73, 27–33. https://doi.org/10.1289/ehp.877327.

Michie, K.A., Bermeister, A., Robertson, N.O., Goodchild, S.C., Curmi, P.M.G., 2019. Two sides of the coin: Ezrin/Radixin/Moesin and Merlin control membrane structure and contact inhibition. Int J. Mol. Sci. 20, 1996. https://doi.org/10.3390/ijms20081996.

Muriel, O., Tomas, A., Scott, C.C., Gruenberg, J., 2016. Moesin and cortactin control actin-dependent multivesicular endosome biogenesis. Mol. Biol. Cell 27, 3305–3316. https://doi.org/10.1091/mbc.E15-12-0853.

Namgoong, S., Kim, N.-G., 2016. Roles of actin binding proteins in mammalian oocyte maturation and beyond. Cell Cycle 15, 1830–1843. https://doi.org/10.1080/15384101.2016.1181239.

Nishimura, T., Araki, H., Higuchi, K., Noguchi, S., Saito, K., Hara, K., Yagishita, H., Akashi, R., Obata, S., Tomi, M., 2024. Involvement of GAT2/Slc6a13 in hypotaurine uptake at fetal-facing plasma membrane of syncytiotrophoblasts at mid-to-late gestation in rats and mice. Placenta 147, 59–67. https://doi.org/10.1016/j.placenta.2024.01.017.

Polesello, C., Delon, I., Valenti, P., Ferrer, P., Payre, F.D., 2002. Moesin controls actin-based cell shape and polarity during Drosophila melanogaster oogenesis. Nat. Cell Biol. 4, 782–789. https://doi.org/10.1038/ncb856.

Ponuwei, G.A., 2016. A glimpse of the ERM proteins. J. Biomed. Sci. 23, 35. https://doi.org/10.1186/s12929-016-0246-3.

Roelen, B.A.J., 2020. Bovine oocyte maturation: acquisition of developmental competence. Reprod. Fertil. Dev. 32, 98–103. https://doi.org/10.1071/RD19255.

Romeis, B., 1989. Mikroskopische Technik. 17th ed. Urban and Schwarzenberg, Munich-Vienna-Baltimore.

Saotome, I., Curto, M., McClatchey, A.I., 2004. Ezrin is essential for epithelial organization and villus morphogenesis in the developing intestine. Dev. Cell 6, 855–864. https://doi.org/10.1016/j.devcel.2004.05.007.

Schön, M., Mey, I., Steinem, C., 2019. Influence of cross-linkers on ezrin-bound minimal actin cortices. Prog. Biophys. Mol. Biol. 144, 91–101. https://doi.org/10.1016/j.pbiomolbio.2018.07.016.

Smith, M.F., McIntush, E.W., Smith, G.W., 1994. Mechanisms associated with corpus luteum development. J. Anim. Sci. 72, 1857–1872. https://doi.org/10.2527/1994.7271857x.

Storr, S.J., Hoskin, V., Aiyappa-Maudsley, R., Ghaffari, A., Varma, S., Green, A., Rakha, E., Ellis, I.O., Greer, P.A., Martin, S.G., 2023. A retrospective analysis of ezrin protein and mRNA expression in breast cancer: Ezrin expression is associated with patient survival and survival of patients with receptor-positive disease. Cancer Med 12, 10908–10916. https://doi.org/10.1002/cam4.5802.

Tabrizi, M.E.A., Gupta, J.K., Gross, S.R., 2023. Ezrin and its phosphorylated Thr567 form are key regulators of human extravillous trophoblast motility and invasion. Cells 12, 711. https://doi.org/10.3390/cells12050711.

Tsukita, S., Yonemura, S., 1999. Cortical actin organization: lessons from ERM (ezrin/radixin/moesin) proteins. J. Biol. Chem. 274, 34507–34510. https://doi.org/10.1074/jbc.274.49.34507.

Walter, I., Burger, S., Stargardt, M., Kummer, S., Wieser, M., 2020. VetBiobank, vetmeduni vienna: a bioresource for clinical animal biospecimens. Open J. Bioresour. 7, 9. https://doi.org/10.5334/ojb.60.

Wan, T., Sun, H., Mao, Z., Zhang, L., Chen, X., Shi, Y., Shang, Y., 2021. Vitamin D deficiency inhibits microRNA-196b-5p which regulates ovarian granulosa cell hormone synthesis, proliferation, and apoptosis by targeting RDX and LRRC17. Ann. Transl. Med 9, 1775. https://doi.org/10.21037/atm-21-6081.

Wang, S., Jiao, B., Geng, S., Song, J., Liang, Lu, S., 2014. Concomitant microRNA-31 downregulation and radixin upregulation predicts advanced tumor progression and unfavorable prognosis in patients with gliomas. J. Neurol. Sci. 338, 71–76. https://doi.org/10.1016/j.jns.2013.12.019.

Yu, L., Zhao, L., Wu, H., Zhao, H., Yu, Z., He, M., Jin, F., Wei, M., 2019. Moesin is an independent prognostic marker for ER-positive breast cancer. Oncol. Lett. 17, 1921–1933. https://doi.org/10.3892/ol.2018.9799.

Zachos, N.C., Burch, M.G., Billiar, R.B., Li, C., Albrecht, E.D., Pepe, G.J., 2008. Regulation of expression of microvillus membrane proteins by estrogen in baboon fetal ovarian oocytes. Biol. Reprod. 79, 1160–1168. https://doi.org/10.1095/biolreprod.108.067900.

Zhang, S., Dolgalev, I., Zhang, T., Ran, H., Levine, D.A., Neel, B.G., 2019. Both fallopian tube and ovarian surface epithelium are cells-of-origin for high-grade serous ovarian carcinoma. Nat. Commun. 10, 5367. https://doi.org/10.1038/s41467-019-13116-2.

Zhang, Y., Wang, Y., Feng, X., Zhang, S., Xu, X., Li, L., Niu, S., Bo, Y., Wang, C., Li, Z., Xia, G., Zhang, H., 2021. Oocyte-derived microvilli control female fertility by optimizing ovarian follicle selection in mice. Nat. Commun. 12, 2523. https://doi.org/10.1038/s41467-021-22829-2.

Zhao, L.-P., Huang, L., Tian, X., Liang, F.-Q., Wei, J.-C., Zhang, X., Li, S., Zhang, Q.-H., 2016. Knockdown of ezrin suppresses the migration and angiogenesis of human umbilical vein endothelial cells *In Vitro*. J. Huazhong Univ. Sci. Technol. 36, 243–248. https://doi.org/10.1007/s11596-016-1574-y.

Zhuan, Q., Li, J., Du, X., Zhang, L., Meng, L., Luo, Y., Zhou, D., Liu, H., Wan, P., Hou, Y., Fu, X., 2022. Antioxidant procyanidin B2 protects oocytes against cryoinjuries via mitochondria regulated cortical tension. J. Anim. Sci. Biotechnol. 13, 95. https://doi.org/10.1186/s40104-022-00742-y.